Vítor Monteiro, J. G. Pinto, J. C. Aparício Fernandes, João L. Afonso,

"Experimental Comparison of Single-Phase Active Rectifiers for EV Battery Chargers"

VEHITS International Conference on Vehicle Technology and Intelligent Transport Systems, Porto Portugal, pp.419-425, Abr. 2017.

ISBN: 978-989-758-242-4

Vítor Monteiro, J. G. Pinto, J. C. Aparício Fernandes, João L. Afonso, "Experimental Comparison of Single-Phase Active Rectifiers for EV Battery Chargers", VEHITS International Conference on Vehicle Technology and Intelligent Transport Systems, Porto Portugal, pp.419-425, Abr. 2017. ISBN 978-989-758-242-4

Experimental Comparison of Single-Phase Active Rectifiers for EV Battery Chargers

Vítor Monteiro, J. G. Pinto, J. C. Aparício Fernandes, and João L. Afonso
University of Minho, Campus de Azurem, Guimarães, Portugal
{vitor.monteiro, gabriel.pinto, aparicio.fernandes, joao.l.afonso}@algoritmi.uminho.pt

Keywords: Active Rectifier, Battery Charger, Electric Vehicle, Power Quality.

Abstract: An experimental comparison of single-phase active rectifiers for electric vehicle (EV) battery chargers is presented and discussed. Active rectifiers are used in on-board EV battery chargers as front-end converters to interface the power grid aiming to preserve the power quality. In this paper, four topologies of active rectifiers are compared: traditional power-factor-correction; symmetrical bridgeless; asymmetrical bridgeless; and full-bridge full-controlled. Such comparison is established in terms of the requirements for the hardware structure, the complexity of the digital control system, and the power quality issues, mainly the grid current total harmonic distortion and the power factor. Along the paper these comparisons are presented and verified through experimental results. A reconfigurable laboratorial prototype of an on-board EV battery charger connected to the power grid was used to obtain the experimental results.

1 INTRODUCTION

The acceptance of the electric vehicle (EV) around the world, represents a new paradigm for the transportation sector and for the actual and future power grids (Rajashekara, 2013)(Raghavan, 2012). Nevertheless, a full electric mobility scenario is a huge challenge that is dependent of key technological issues (Ferreira, 2014)(Khaligh, 2010)(Inoa, 2011). From the point of view of the transportation sector, the EV contributes significantly to reduce the greenhouse gas emissions, mainly through the reduction of the oil consumption (Milberg, 2011)(Ferreira, 2013). However, it depends on the main electricity sources (Ferreira, 2013). On the other hand, from the point of view of the power grids, the EV represents a new type of dynamic electrical appliance that is plugged-in to consume energy randomly along the day. Moreover, the EV can contribute to worse the power quality (Lopes, 2011)(Wirasingha, 2011)(Monteiro, 2016). Analysing this last aspect, and taking into account the global state of the electric mobility, the EV should be charged from the power grid considering the electrical installation constrains and with high levels of power quality, mainly, reduced current harmonic distortion and high power factor (Monteiro, 2011). Such requirements should be considered for on-board and off-board EV chargers (Gautam, 2012)(Monteiro, 2014), i.e., when the EV is charged from single-phase electrical installations (e.g., plugged-in at home) or from three-phase electrical installations (e.g., plugged-in at fast charging stations) (Clement, 2010). Besides the charging process, from the moment that the EV is plugged-in to the power grid, using bidirectional chargers is possible establish a bidirectional energy flow, i.e., the EV can dynamically operate in the power grid consuming or delivering energy (Kramer, 2008)(Monteiro, 2016). This interactivity with the power grid is an important key technology to enable the electric mobility into smart grids (Monteiro, 2010)(Escudero-Garzás, 2012). In this context, technical solutions to the EV introduction into the power grids are presented in (Rei, 2010), coordinated strategies for the EV charging aiming to maximize the efficiency are presented in (Clement, 2009), and a comprehensive analysis about the EV coordinated and uncoordinated charging strategies is presented in (Freire, 2010).

Concerning EV battery chargers, this paper presents an experimental comparison of four active rectifiers for on-board EV battery chargers in terms

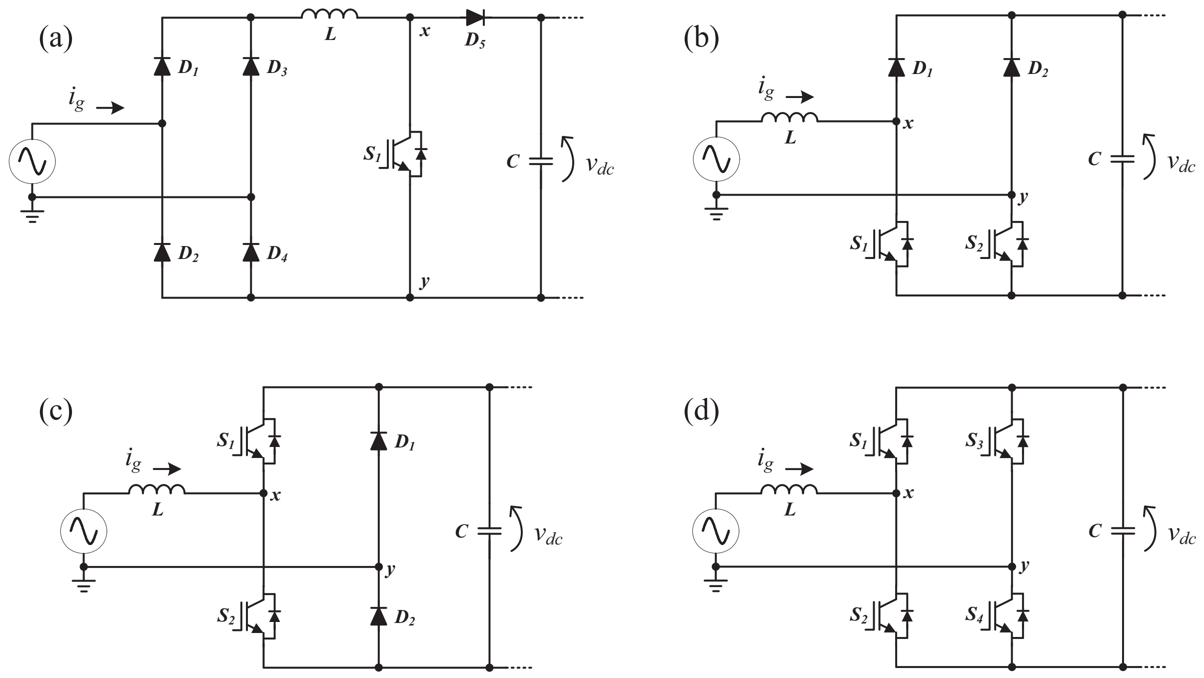

Figure 1: Single-phase active rectifiers under comparison: (a) Traditional power-factor-correction (PFC); (b) Symmetrical bridgeless; (c) Asymmetrical bridgeless; (d) Full-bridge full-controlled.

of power quality, where the current harmonic distortion and the power factor are the main issues addressed. A comparison of dc-dc converters operating in discontinuous conduction mode for active rectifiers is presented in (Wei, 1998), and a comprehensive review of control strategies for active rectifiers considering the main advantages and disadvantages is presented in (Yang, 1998). Active rectifiers are used in EV chargers in order to obtain a sinusoidal grid current in phase with the power grid voltage. However, comparing with the traditional solutions based in the ac-dc diode bridge rectifier, the power hardware is much more complex and requires a digital control platform, increasing the costs and the power density of the implementation. The impact of the EV introduction in residential electrical installations in terms of power quality is presented in (Lambert, 2002). Detailed studies about this subject are presented in (Morcos, 2002), where, for instance, is shown that the GM EV1 presents a total harmonic distortion (THD) that varies from 3% to 28.11% and a power factor from 1 to 0.96 according to the battery state-of-charge.

In this context, the main contribution of this paper is an experimental comparison of single-phase active rectifiers for EV battery chargers. Section II presents the power hardware structure of the active rectifiers under comparison, including a comparison in terms of required components. Section III presents a detailed description of the control algorithms. Section IV presents an experimental validation of all the active rectifiers under comparison. Finally, section V presents the main conclusions that can be retrieved from the presented comparison.

2 HARDWARE STRUCTURE OF THE ACTIVE RECTIFIERS UNDER COMPARISON

This section describes the hardware structure of the active rectifiers under comparison. A reconfigurable 3.6 kW on-board EV battery charger was used to obtain the different structures. Such EV charger is composed by a front-end ac-dc converter and by a back-end dc-dc converter with a shared dc-link capacitor. Figure 1 shows the four single-phase active rectifiers under comparison.

The traditional power-factor-correction (PFC) active rectifier (cf. Figure 1(a)) is composed by full-bridge diode rectifier followed by a boost dc-dc converter. As shown, this active rectifier requires five diodes and a single totally controlled semiconductor, in this case an insulated-gate bipolar transistor (IGBT) is used. The circuit to control the IGBT can be directly connect to the control circuit, i.e., it is not necessary isolation between the power circuit and the control circuit. This can be an important advantage of this active rectifier comparing with the others. The symmetrical bridgeless active rectifier (cf. Figure 1(b)) is composed by two legs, each one formed by a diode and by an IGBT. Similarly to the previous active rectifier, the circuit to control the IGBTs can be directly connect to the control circuit, i.e., it is not necessary isolation between the power circuit and the control circuit, once the emitter of both IGBTs is connected to the same point. On the other hand, the asymmetrical bridgeless active rectifier (cf. Figure 1(c)) is composed by a leg formed by two diodes and by a leg formed by two IGBTs. In this active rectifier is necessary isolation between the drivers circuit of both IGBTs, representing a disadvantage of this active rectifier comparing with the previous. Finally, the full-bridge full-controlled active rectifier (cf. Figure 1(d)) is composed by two legs, each one formed by two IGBTs. In this active rectifier is also necessary to establish isolation between the drivers of the IGBTs, i.e., only the drivers of the IGBTs S_2 an S_4 can be referred to the same point.

3 CONTROL ALGORITHMS OF THE ACTIVE RECTIFIERS UNDER COMPARISON

This section presents a detailed explanation about the control algorithms of the active rectifiers under comparison.

3.1 Traditional Power Factor Correction (PFC)

Concerning power quality, the main requirements of the EV battery chargers are sinusoidal grid current and unitary power factor. The most used active rectifier to accomplish with such requirements is the traditional PFC, i.e., a full-bridge diode rectifier followed by a dc-dc boost converter operating with controlled input current and controlled output voltage. It is important to note that there are some PFC converters that are used only to operate with controlled power factor, as example, the flyback topology proposed in (Ma, 2010) and the full-bridge topology proposed in (Moschopoulos, 2003). An extended review about PFC converters based in the boost converter is presented in (García, 2003), and a concrete case of a PFC boost-type for EV chargers is proposed in (Lee, 2011). The PFC active rectifier operates in unidirectional mode and is classified as a two-level converter, i.e., the voltage between the points x and y, identified in Figure 1(a) can assume the levels 0 and $+v_{dc}$. When the IGBT is off, the voltage v_{xy} (collector-emitter voltage in the IGBT) is $+v_{dc}$, and when the IGBT is on, the voltage v_{xy} is 0. Therefore, the maximum voltage applied to the IGBT is $+v_{dc}$. The output voltage of the full-bridge diode rectifier is the power grid voltage rectified and, due to the input inductance and the control algorithm, the grid current is sinusoidal and in phase with the power grid voltage.

3.2 Symmetrical and Asymmetrical Bridgeless

In the previous item, section 3.1, it was introduced the traditional PFC composed by a full-bridge diode rectifier followed by a dc-dc boost converter, i.e., an active rectifier that requires two power stages. However, these stages can be rearranged in order to form an active rectifier without the full-bridge diode rectifier. Such topologies are identified in the literature as bridgeless or dual-boost. A review about active rectifiers with single stage is presented in (Huber, 2008). The main bridgeless active rectifiers identified in the literature are the symmetrical and asymmetrical (Martinez, 1996)(Lim, 1999). Comparing with the traditional PFC, bridgeless active rectifiers requires one more IGBT, but less three diodes. However, it should be noted that the hardware project of such topologies is more complex once is required the double of the IGBTs drivers. On the other hand, comparing both bridgeless structures, the symmetrical bridgeless has as main advantage comparing with the asymmetrical the simplicity of the IGBTs drivers as well as the impossibility of short circuits in the same leg when both IGBTs are on. A comparison between the symmetrical and the asymmetrical bridgeless active rectifiers, highlighting the benefits of the symmetrical is presented in (Choi, 2007). Comparing with the traditional PFC, the switching losses are very similar once each IGBT is switched during each half-cycle of the power grid voltage (positive and negative) and the IGBT of the traditional PFC is switched in both half-cycles. Similarly to the traditional PFC, symmetrical and the asymmetrical bridgeless active rectifiers operate in unidirectional mode, but can be controlled to produce three distinct voltage levels, i.e., the voltage v_{xy} can assume the values $+v_{dc}$, 0 and $-v_{dc}$. For the symmetrical bridgeless active rectifier, during the positive half-cycle of the power grid voltage, when the IGBT S_1 is on and the IGBT S_2 is off, the voltage v_{xy} is 0, and when both IGBTs are off the voltage v_{xy} is $+v_{dc}$. On the other hand, during the negative half-cycle of the power grid voltage, when the IGBT S_1 is off and the IGBT S_2 is on, the voltage v_{xy} is 0, and when both IGBTs are off the voltage v_{xy} is $-v_{dc}$. For the asymmetrical bridgeless active rectifier the reasoning is the same, only changing the position of the IGBTs. For both converters, the maximum voltage applied to each IGBT is $+v_{dc}$.

3.2 Full-Bridge Full-Controlled

The full-bridge active rectifier is composed by two legs of IGBTs. This active rectifier can produce three distinct voltage levels, i.e., the voltage v_{xy} can assume the values of $-v_{dc}$, 0 and $+v_{dc}$. During the positive half-cycle of the power grid voltage, when the IGBTs S_1 and S_3 are off and the IGBTs S_2 and S_4 are on, the voltage v_{xy} is 0 (changing the state of all the IGBTs the voltage v_{xy} is also 0), and when the IGBTs S_2 and S_3 are off and the IGBTs S_1 and S_4 are on, the voltage v_{xy} is $+v_{dc}$. During the negative half-cycle of the power grid voltage, when the IGBTs S_1 and S_3 are off and the IGBTs S_2 and S_4 are on, the voltage v_{xy} is 0 (changing the state of all the IGBTs the voltage v_{xy} is also 0), and when the IGBTs S_2 and S_3 are on and the IGBTs S_1 and S_4 are off, the voltage v_{xy} is $-v_{dc}$. The maximum voltage applied to each IGBT is v_{dc}. The main advantage of this active rectifier comparing with the previous is the possibility to operate in bidirectional mode, i.e., the EV charger can be used to transfer energy from the batteries to the power grid. This is an important characteristic considering the future scenarios of smart grids.

4 EXPERIMENTAL VALIDATION

This section presents the experimental validation considering the active rectifiers described in the previous items. The reconfigurable laboratorial prototype of the on-board EV battery charger used to obtain the experimental results is shown in Figure 2, and the main characteristics of the experimental validation are presented in table I. The experimental results were obtained in laboratorial environment with a *Tektronix TPS 2024* digital oscilloscope.

For the traditional PFC active rectifier, Figure 3 shows the power grid voltage (v_g), the dc-link voltage (v_{dc}), and the grid current (i_g) during a time interval of 50 ms. As expected, the grid current (i_g) is sinusoidal and in phase with the power grid voltage (v_g), and the dc-link voltage (v_{dc}) is controlled. As it can be seen, the grid current (i_g) has lower THD% than the power grid voltage (v_g) due to the control algorithm, i.e., instead of use the real instantaneous values of power grid voltage a phase-locked loop (PLL) algorithm is used. Figure 4 shows the harmonic spectrum of the grid current and a measured THD% of 3.25%.

For the symmetrical bridgeless active rectifier, Figure 5 shows the power grid voltage (v_g), the dc-link voltage (v_{dc}), and the grid current (ig) during a time interval of 50 ms. As for the previous active rectifier, the grid current (i_g) is sinusoidal and in phase with the power grid voltage (v_g), and the dc-link voltage (v_{dc}) is controlled. In this case, the grid current (i_g) has also lower THD% than the power grid voltage (v_g) due to the PLL algorithm. Nevertheless, in this case grid current (i_g) has a

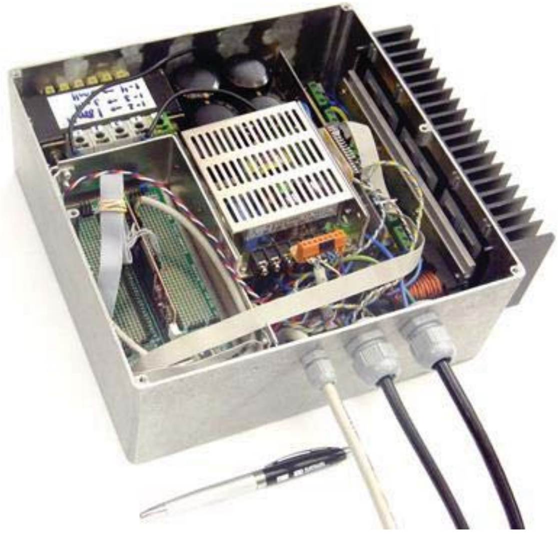

Figure 2: Reconfigurable laboratorial prototype of the on-board EV battery charger used to obtain the experimental results.

Table I: Main characteristics of the developed laboratorial prototype used for experimental validation.

Characteristic	Value	Unit
Switching frequency	20	kHz
Sampling frequency	40	kHz
Power grid voltage	50	V
Power Grid Voltage THD%	3%	-
Power grid frequency	50	Hz
Output voltage	100	V

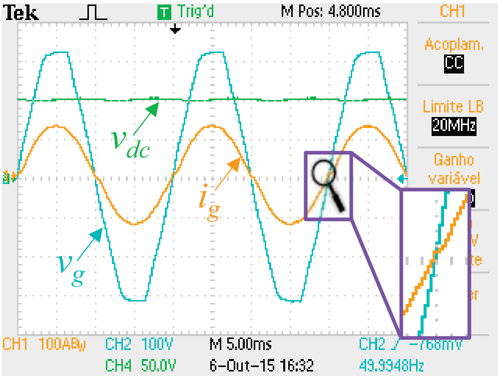

Figure 3: Experimental results of the traditional power factor correction topology: Power grid voltage (v_g); Dc-link voltage (v_{dc}); Grid current (i_g).

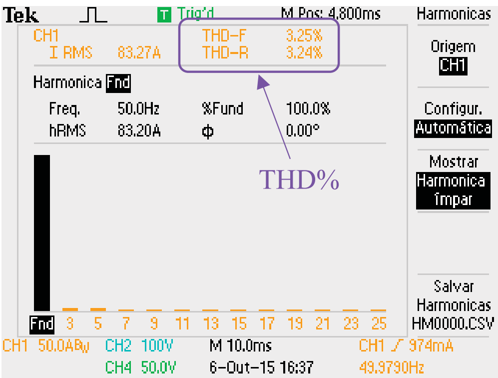

Figure 4: Experimental results of the traditional power factor correction topology: Harmonic spectrum of the grid current and measured THD%.

THD% greater than with the traditional PFC active rectifier. Figure 6 shows the harmonic spectrum of the grid current and a measured THD% of 5.88%. For the asymmetrical bridgeless active rectifier,

Figure 7 shows the power grid voltage (v_g), the dc-link voltage (v_{dc}), and the grid current (i_g) during a time interval of 50 ms. Similarly to the previous case, the grid current (i_g) is sinusoidal and in phase with the power grid voltage (v_g), the dc-link voltage (v_{dc}) is controlled, and the grid current (i_g) has lower THD% than the power grid voltage (v_g) due to the PLL algorithm. Comparing with the symmetrical bridgeless active rectifier, this active rectifier presents a grid current (i_g) with higher THD%.

Figure 8 shows the harmonic spectrum of the grid current and a measured THD% of 5.98%. Finally, for the full-bridge active rectifier, Figure 9 shows the power grid voltage (v_g), the dc-link voltage (v_{dc}), and the grid current (ig) during a time interval of 50 ms. In the same way as the previous cases, the grid current (i_g) is sinusoidal and in phase

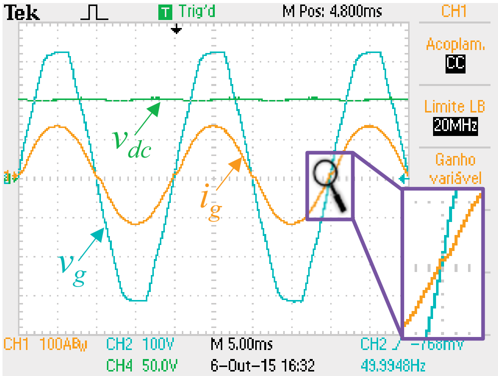

Figure 5: Experimental results of the symmetrical bridgeless topology: Power grid voltage (v_g); Dc-link voltage (v_{dc}); Grid current (i_g).

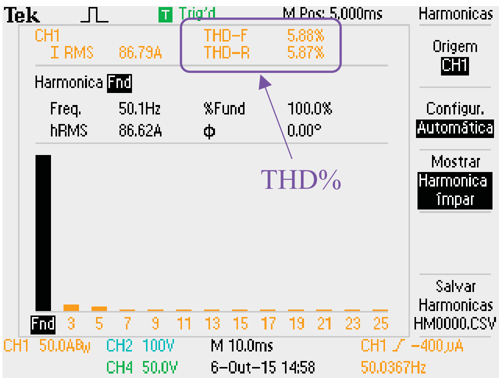

Figure 6: Experimental results of the symmetrical bridgeless topology: Harmonic spectrum of the grid current and measured THD%.

with the power grid voltage (v_g), the dc-link voltage (v_{dc}) is controlled, and the grid current (i_g) has lower THD% than the power grid voltage (v_g) due to the PLL algorithm. The grid current (i_g) of this active rectifier presents the lower THD% considering all the active rectifiers under comparison. Figure 10 shows the harmonic spectrum of the grid current and a measured THD% of 2.13%.

5 CONCLUSIONS

An experimental comparison of single-phase active rectifiers for EV battery chargers was presented. Four topologies of active rectifiers were considered for comparison: traditional power factor correction (PFC); symmetrical bridgeless; asymmetrical bridgeless; and full-bridge full-controlled. Considering the hardware structure, the PFC requires less IGBTs, but more diodes, and the full-bridge full-controlled requires more IGBTs but

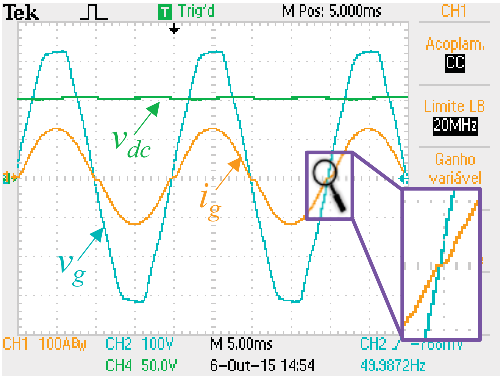

Figure 7: Experimental results of the asymmetrical bridgeless topology: Power grid voltage (v_g); Dc-link voltage (v_{dc}); Grid current (i_g).

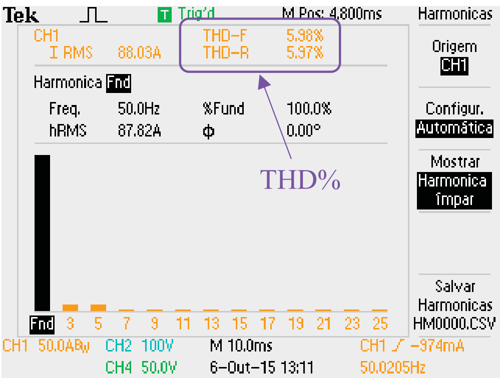

Figure 8: Experimental results of the asymmetrical bridgeless topology: Harmonic spectrum of the grid current and measured THD%.

no one diode. Moreover, the full-bridge full-controlled allows the operation mode in bidirectional mode, which can be an important feature for EV battery chargers in a smart grid scenario. Analysing the power quality issues in terms of the grid current THD%, the full-bridge full-controlled is the best, presenting the lower value (2.13%), and the bridgeless asymmetrical is the worst, presenting the higher value (5.98%). Along the paper the comparison between the active rectifiers is presented through experimental results using a reconfigurable developed laboratorial prototype of an on-board EV battery charger.

ACKNOWLEDGEMENTS

This work has been supported by COMPETE: POCI-01-0145-FEDER-007043 and FCT – Fundação para a Ciência e Tecnologia within the

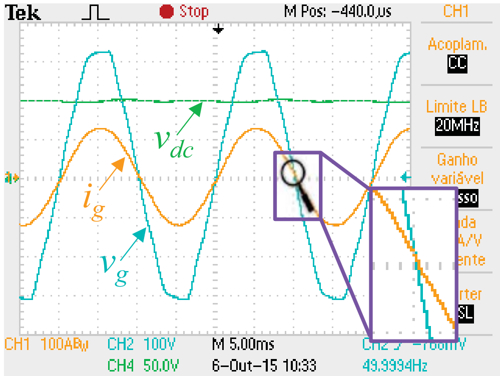

Figure 9: Experimental results of the full-bridge full-controlled topology: Power grid voltage (v_g); Dc-link voltage (v_{dc}); Grid current (i_g).

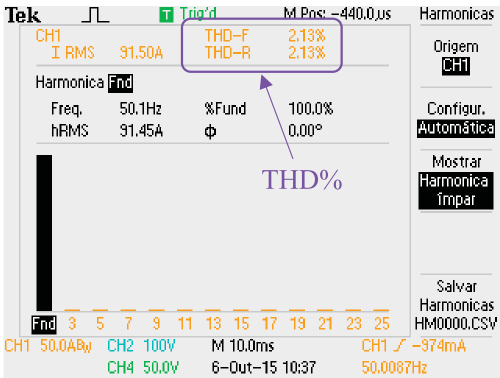

Figure 10: Experimental results of the full-bridge full-controlled topology: Harmonic spectrum of the grid current and measured THD%.

Project Scope: UID/CEC/00319/2013. This work is financed by the ERDF – European Regional Development Fund through the Operational Programme for Competitiveness and Internationalisation - COMPETE 2020 Programme, and by National Funds through the Portuguese funding agency, FCT - Fundação para a Ciência e a Tecnologia, within project SAICTPAC/0004/2015-POCI- 01-0145-FEDER-016434.

REFERENCES

Clement, K., Haesen, E., Driesen, J., (2010). The Impact of Charging Plug-In Hybrid Electric Vehicles on a Residential Distribution Grid. *IEEE Trans. on Power Systems*.

Clement, K., Haesen, E., Driesen, J., (2009). Coordinated charging of multiple plug-in hybrid electric vehicles in residential distribution grids. *PSCE Power Systems Conference and Exposition*.

Choi, W. Y., Kwon, J. M., Kim, E. H., Lee, J. J., Kwon, B. H., (2007). Bridgeless Boost RectifierWith Low Conduction Losses and Reduced Diode Reverse-Recovery Problems. *IEEE Trans. on Industrial Electronics*.

Escudero-Garzás, J. J., García-Armada, A., Seco-Granados, G., (2012). Fair Design of Plug-in Electric Vehicles Aggregator for V2G Regulation. *IEEE Trans. on Vehicular Technologies*.

Ferreira, J. C., Monteiro, V., Afonso, J. L., (2014). Vehicle-to-Anything Application (V2Anything App) for Electric Vehicles. *IEEE Trans. on Industrial Informatics*.

Ferreira, J. C., Monteiro, V., Afonso, J. L., (2013). Dynamic range prediction for an electric vehicle. EVS*27 Electric Vehicle Symposium and Exhibition*.

Ferreira, J. C., Silva, A. R., Monteiro, V., Afonso, J. L., (2013). Collaborative Broker for Distributed Energy Resources. *Conference on Computational Intelligence and Decision Making*.

Freire, R., Delgado, J., Santos, J. M., Almeida, A. T., (2010). Integration of Renewable Energy Generation with EV Charging Strategies to Optimize Grid Load Balancing. *IEEE Conference on Intelligent Transportation Systems*.

Gautam, D. s., Musavi, F., Edington, M., Eberle, W., Dunford, W. g., (2012). An Automotive Onboard 3.3-kW Battery Charger for PHEV Application. *IEEE Trans. on Vehicular Technologies*.

García, O., Cobos, J. A., Prieto, R., Alou, P., Uceda, J., (2003). Single Phase Power Factor Correction: A Survey. *IEEE Trans. on Power Electronics*.

Huber, L., Jang, Y., Jovanovic, M., (2008). Performance Evaluation of Bridgeless PFC Boost Rectifier. *IEEE Trans. on Power Electronics*.

Inoa, E., Wang, J., (2011). PHEV Charging Strategies for Maximized Energy Saving. *IEEE Trans. on Vehicular Technologies*.

Khaligh, A., Li, Z.,(2010). Battery, Ultracapacitor, Fuel Cell, and Hybrid Energy Storage Systems for Electric, Hybrid Electric, Fuel Cell, and Plug-In Hybrid Electric Vehicles: State of the Art. *IEEE Trans. on Vehicular Technologies*.

Kramer, B., Chakraborty, S., Kroposki, B., (2008). A review of plug-in vehicles and vehicle-to-grid capability. *IEEE IECON Industrial Electronics Conference*.

Lee, C. S., Jeong, J. B., Lee, B. H., Hur, J., (2011). Study on 1.5 kW Battery Chargers for Neighborhood Electric Vehicles. *IEEE VPPC Vehicle Power and Propulsion Conference*.

Lambert, F., (2002). Secondary Distribution Impacts of Residential Electric Vehicle Charging. *California Energy Commission*.

Lopes, J. A. P., Soares, F., Almeida, P. M. R., (2011). Integration of Electric Vehicles in the Electric Power Systems. *Proceedings of the IEEE*.

Lim, J. W., Kwon, B. H., (1999). A Power-Factor Controller for Single-Phase PWM Rectifiers. *IEEE Trans. on Industrial Electronics*.

Moschopoulos, G., (2003). A Simple AC–DC PWM Full-Bridge Converter With Integrated Power-Factor Correction. *IEEE Trans. on Power Electronics*.

Ma, H., Ji, Y., Xu, Y., (2010). Design and Analysis of Single-Stage Power Factor Correction Converter With a Feedback Winding. *IEEE Trans. on Power Electronics*.

Milberg, J., Ann Schlenker, A., (2011). Plug into the Future. *IEEE Power and Energy Magazine*.

Martinez, R., Enjeti, P. N., (1996). A High-Performance Single-phase Rectifier with Input Power Factor Correction. *IEEE Trans. on Power Electronics*.

Morcos, M., Dillman, N., Mersman, C., (2002). Battery Chargers for Electric Vehicles. *IEEE Power Engineering Review*.

Monteiro, V., Gonçalves, H., Afonso, J. L., (2011). Impact of Electric Vehicles on Power Quality in a Smart Grid Context. *IEEE EPQU International Conference on Electrical Power Quality and Utilisation*.

Monteiro, V., Exposto, B., Pinto, J. G., Almeida, R., Ferreira, J. C., Meléndez, A. A. N., Afonso, J. L., (2014). On-Board Electric Vehicle Battery Charger with Enhanced V2H Operation Mode. *IEEE IECON Industrial Electronics Conference*.

Monteiro, V., Ferreira, J. C., Pinto, J. G., Pedrosa, D., Afonso, J. L., (2010). iV2G Charging Platform. *IEEE ITSC International Conference on Intelligent Transportation Systems*.

Monteiro, V., Ferreira, J. C., Meléndez, A. A. N., Afonso, J. L., (2016). Model predictive control applied to an improved five-level bidirectional converter. *IEEE Transactions on Industrial Electronics*.

Monteiro, V., Exposto, B., Ferreira, J. C., Afonso, J. L., (2016). Improved vehicle-to-home (iV2H) operation mode: experimental analysis of the electric vehicle as off-line UPS. *IEEE Trans. on Smart Grid*.

Rajashekara, K., (2013). Present Status and Future Trends in Electric Vehicle Propulsion Technologies. *IEEE Journal of Emerging and Selected Topics in Power Electronics*.

Rei, R. J., Soares, F. J., Almeida, P. M. R., Lopes, J. A. P., (2010). Grid Interactive Charging Control for Plug-in Electric Vehicles. *IEEE Conference on Intelligent Transportation Systems*.

Raghavan, S. S., Khaligh, A., (2012). Electrification Potential Factor: Energy-Based Value Proposition Analysis of Plug-In Hybrid Electric Vehicles. *IEEE Trans. on Vehicular Technologies*.

Wirasingha, S. G., Emdai, A., (2011). Classification and Review of Control Strategies for Plug-In Hybrid Electric Vehicles. *IEEE Trans. on Vehicular Technologies*.

Wei, H., Batarseh, I., (1998). Comparison of basic converter topologies for power factor correction. *IEEE Southeastcon Proceedings*.

Yang, Z., Sen, P. C., (1998). Recent developments in high power factor switchmode converters. *IEEE Canadian Conference on Electrical and Computer Engineering*.